International Journal of Innovative Computing, Information and Control
Volume **20**, Number **2**, April **2024**

ICIC International ©2024 ISSN 1349-4198
pp. 411–435

EVALUATION OF PRODUCTION SYSTEMS FROM A NEW PERSPECTIVE OF SPIN GLASS THEORY IN STATISTICAL MECHANICS

Kenji Shirai[1], Yoshinori Amano[2], Atsuya Ando[1] and Takayuki Uda[1]

[1]Faculty of Business and Informatics
Niigata University of International and Information Studies
3-1-1, Mizukino, Nishi-ku, Niigata 950-2292, Japan
dr.kenji5761@gmail.com; { atsuya; uda }@nuis.ac.jp

[2]Kyohnan Elecs Co., Ltd.
8-48-2, Fukakusanishiura-cho, Fushimi-ku, Kyoto 612-0029, Japan
y_amano@kyohnan-elecs.co.jp

Received June 2023; revised October 2023

Abstract. *The most important thing in the Spin Glass Theory is that it theoretically explains the phenomenon called the spin glass effect. The spin glass effect is a phenomenon in which the optical properties of an object change when it is rotated, such as reflecting or transmitting light. First, our focus was on the fact that Edwards-Anderson model can be utilized to link the work time required by workers in each process to the time taken over to the next process in the production process. Ferromagnetic order is an order in which spins align in the same direction, and magnetization is the order parameter that defines it. We analyze the production density flowing through the production process in relation to order variables. As a mathematical model, an advection-diffusion equation is introduced. Therefore, we consider that ferromagnetic order corresponds to production density. The average value for the free energy of Edwards-Anderson model corresponds to considering the interaction between adjacent processes on a process-by-process basis.*
Keywords: Spin Glass Theory, Spin glass order parameter, Free-energy Landscape, Gaussian distribution, Production processes

1. **Introduction.** A motive that the present writers and the like started to promote such kind of research during many years of experience of manufacturing operations of control equipment for general industrial machines is as follows. In our previous studies, all angles reported that schemes with superior rates of return were better synchronous processes than asynchronous processes. As a major contribution, we have proposed measures to improve the efficiency of production systems, backed by mathematical models of deterministic which is the advection-type diffusion equation, and stochastic systems which is lognormal-type stochastic differential equation [1, 2, 3, 4]. There are reports based on analytical mechanics, arguments in Riemannian space and general relativity to demonstrate the superiority of synchronous production processes [5, 6, 7, 8, 9]. The process that concretely realizes the synchronous production system is called the production flow system. The production flow system is presented with real data in all the papers we have proposed. Also, the previous research applying fluid mechanics to the trial production of a new concept vertical take-off and landing rotorcraft of flexible kite wing attached multicopter is very interesting [11].

DOI: 10.24507/ijicic.20.02.411

In Spin Glass Theory, the spins of atomic and molecular particles are the focus. Spin glasses are a group of materials that exhibit behavior different from that of normal magnets due to the inhomogeneity of interactions caused by impurities in the alloy. In this case, spin is thought to represent the natural behavior of particles [12, 13, 14]. In this case, we consider the critical state due to phase transition when economic factors particles with irregular interactions, which are assumed to have spin and impurities, are considered using the Spin Glass Theory for complex systems such as those mentioned above. Here, it is assumed that there is no translational symmetry in the field and that there are many candidates for order in the potential. Here, translational symmetry means that it is symmetric with respect to translational operation (parallel movement). For example, from a capitalist perspective, it may contain socialist elements or self-sufficient elements that are considered impurities. Similarly, it can be thought to have the same meaning as containing capitalist free market elements that are considered impurities within socialism.

In our previous research, we proposed that the most effective way to improve productivity in production processes is to use a synchronous production process that minimizes variability. We present this using the Spin Glass Theory to demonstrate the superiority of the synchronous production process. Finally, based on real data, the superiority of the synchronous production process utilizing the Spin Glass Theory is presented. Our focus is on the irregular interactions of a spin-bearing particle ensemble in an impure particle-mixed field.

Impurities can be thought of as elements that determine the unnatural characteristics of particles. For example, from a capitalist perspective, elements of socialism or self-sufficiency that may be seen as impurities may be included [12, 13, 14]. Similarly, it can be thought that there may be elements of capitalism, such as a free market, within socialism that may be seen as impurities. When considering phase transitions and critical states due to spin glasses with irregular interactions, assuming that economic factor particles with spins have impurities and are subject to complex systems as mentioned above, we assume that there is no translational symmetry in the field and that there are many candidates for order in the potential. Here, translational symmetry means that it is symmetric with respect to translational operations (parallel movement).

The most important contribution made by Spin Glass Theory academically is the theoretical explanation of the phenomenon known as the spin glass effect. The spin glass effect is the phenomenon in which the optical properties of an object change when it is rotated, such as reflecting or transmitting light. In the theory of spin glasses, there exists something called a state function. This state function is a function that represents the state of the system and cannot be calculated. Trotter-Suzuki approximation is used as an approximation. The Trotter-Suzuki approximation divides the state function and calculates it.

The flow of the entire paper is as follows.

- Section 2 describes as follows. The outline of the Spin Glass Theory is described. Five realistic assumptions are also made in utilizing Spin Glass Theory. These assumptions are necessary to apply the theory to production processes.
- Section 3 is the formation of the order parameter and free energy for the application of Spin Glass Theory to the production process. This will lead to the application of Spin Glass Theory to production processes in the next section. Specifically, the Ising model is introduced in order to make the target system more understandable. The spin-spin interaction is specified by the exchange interaction called the RKKY (Ruderman-Kittel-Kasuya-Yosida) interaction. This is the formulation on which RKKY bases its application of Spin Glass Theory to the production process. We simulate the

formulation of magnetic susceptibility, order parameters, and free energy landscapes. Here we introduce the mean-field approximation. The mean-field approximation, including order parameters and free energies, is used in the analysis.

- Section 4 describes that the order parameter and the entropy represent the numerical analysis by using the Gaussian integral. Specifically, calculate order parameter and entropy values based on the average and volatility values of the asynchronous production system (Testrun1) and the synchronous production system (Testrun2). The results show that the synchronous production system is superior to the asynchronous production system in terms of production efficiency.
- Section 5 describes the production system in manufacturing equipment industry studied in this paper. This is not a special system, but "Make-to-order system with version control". The production flow system is also a production system that we have created based on the know-how we have accumulated over the years.
- Section 6 summarizes the whole paper and indicates the future research.

See Appendix B and Appendix C for an overview of the graphs and equations in the manuscript except those in Appendix A.

2. Outline of the Spin Glass Theory.

The outline of the Spin Glass Theory is a theory that explains the behavior of magnetic materials that have randomness in their magnetic properties. It is based on the concept of spin glass, which is a type of disordered magnetic material. The theory describes the behavior of these materials in terms of their energy states, and how they interact with each other. It also explains the effects of temperature and external magnetic fields on the behavior of these materials.

Assumptions for utilizing Spin Glass Theory are as follows [12, 13, 14].

- There are sites that include "impurities" as one of the components of the relationship.
- The interaction between sites is irregular and follows a Gaussian distribution.
- The magnetization of ferromagnetic materials has a nonlinear characteristics to temperature.
- The equilibrium state is equivalent to the ordered phase having Free-energy Landscape with respect to J_{ij} as a variation of free energy.
- Replica method is a method of representing n spin glass order phases obtained as Free-energy Landscape as one system by preparing replicas (copies) for each of them and expressing the partition function as Z^n.

Based on the discussion up to this point, the particles in an economic field are connected to each other and interact with each other. Therefore, we assume a system in which these particles have "spins" and contain impurities, and these are distributed irregularly. According to Bloch's Impurity Principle, impurities present in a ferromagnetic material can alter its magnetic properties. According to Hogeeson, in complex systems, due to the high diversity, it is impossible to manage with only pure particles [15].

Figure 1 shows the model diagram representing the binding and spin of each particle, which can be discussed using the Spin Glass Theory. The circles of i, j represent economic factor particles with spin. There is an irregular mutual interaction between i and j. Figure 2 shows that randomly oriented spins cause antiferromagnetic interactions. The black dots indicate impurities. We consider this using the Spin Glass Theory. It is thought that spin represents the natural characteristics of the particle's behavior. Therefore, here we consider the interaction of spins in a field with impurities in the particles, which reflects the probabilistic and irregular nature of the particle's behavior. At this time, impurities are considered to be those that determine the unnatural characteristics of particles. For example, from a capitalist perspective, it may contain socialist elements or self-sufficient

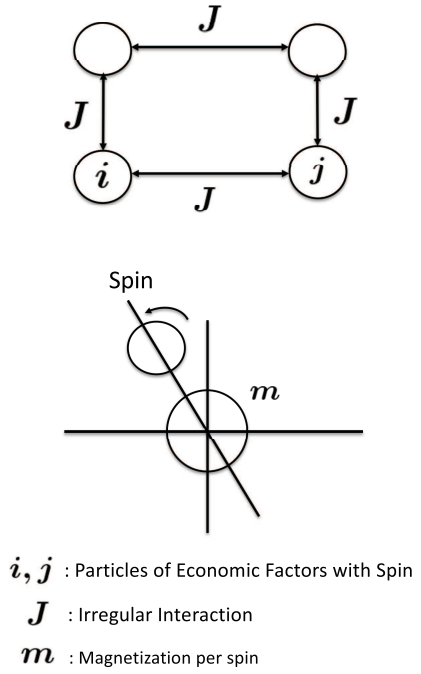

FIGURE 1. State of spin coordination

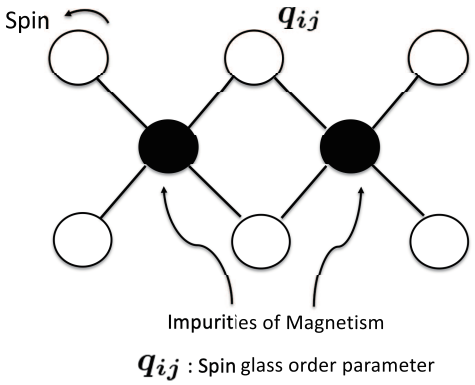

FIGURE 2. Spin table

elements that are considered impurities. Similarly, it can be thought to have the same meaning as containing capitalist free market elements that may be considered impurities within socialism.

Assuming that there are economic factor particles with irregular interactions that have spins and impurities are present, using the Spin Glass Theory, we consider the critical state due to phase transition in complex systems such as those mentioned above. However, it is known that there is no translational symmetry in the field and there are many candidates for order in the potential. "Parallel symmetry" means that it is symmetrical with respect to parallel operations.

Figure 3 is an example of a spin configuration in a ferromagnetic material. Therefore, in Section 3, we consider the density (physical quantity) averaged at each site (magnetic field point) in the Ising model. Figure 4 shows a Free-energy Landscape. The m^1, m^2 and m^N indicate multiple ordered states, where the vertical axis is the free energy and the horizontal axis is the reaction coordinate [12, 13, 14].

3. **Ising Model.**

3.1. **Ruderman-Kittel-Kasuya-Yosida (RKKY) interaction.** Consider the Ising spin model in which spins with positive or negative directions are placed on a 3D cubic lattice. The microscopic state of the system consisting of N spins can be specified by the set $S = (S_1, S_2, \ldots, S_N)$, where the Ising variable $S_i = \pm 1$ represents the sign of the orientation of the lattice point i. In a system where spins are distributed irregularly, the spin-spin interaction J_{ij} takes different values depending on the distance between spins. The Ruderman-Kittel-Kasuya-Yosida (RKKY) interaction is a type of exchange interaction obtained as a spin-spin interaction [12, 13, 14].

$$J_{ij} \sim \frac{\cos(2k_F r_{ij})}{r_{ij}^3} \tag{1}$$

where, the distance between site i and site j is represented by r_{ij}, and k_F is the Fermi wave number. J_{ij} is assumed to have a Gaussian distribution, yielding the following equation.

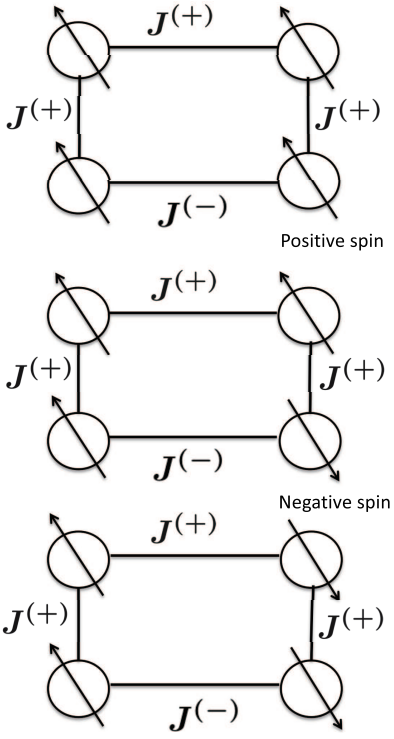

FIGURE 3. An example of a spin arrangement in a ferromagnetic material

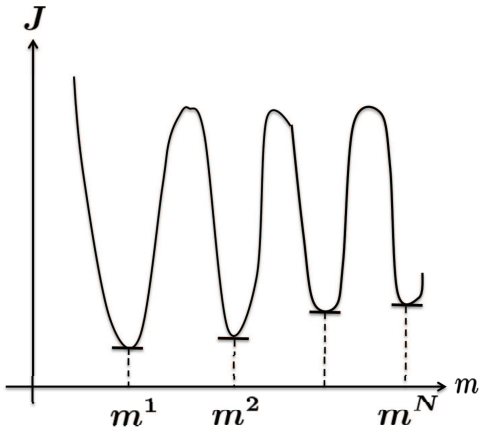

FIGURE 4. Free-energy Landscape

This type of spin model is called the Edwards-Anderson model. The probability distribution at this point is the Gaussian distribution as follows. Equation (1) can be used to link the time required by the workers in each process of the production process with the time for transferring the work to the next process. Therefore, Equation (1) is an important relation for the application of production process analysis. The RKKY interaction is a relatively long-range interaction that is inversely proportional to the cube of the distance, but without taking account of such effects, only the nearest-neighbor interaction is considered. Hamiltonian H of this status is

$$H = -\sum_{\{i,j\}} J_{ij} S_i S_j \tag{2}$$

where S refers to atoms or molecules, and currently $1, 2, \ldots, N$ of them are assumed. $S = (S_1, S_2, \ldots, S_N)$ represents the microscopic state of the entire system consisting of N spins [12, 13, 14].

The model in which J_{ij} takes irregular values is called the Edwards-Anderson model. It is common to take J_{ij} to be a Gaussian distribution with a probability of positive and negative values $\pm J$. By making use of the statistical nature of the Hamiltonian, we considered calculating thermodynamic functions. Many thermodynamic functions are expressed as an average density with respect to sites. This approach is also used in production processes.

$$f = \frac{1}{N} \sum_{i=1}^{N} f_i \tag{3}$$

where f_i is the function of an N-element system, related to each element of the system. f is the average of f_i [12, 13, 14].

Since J_{ij} takes different values depending on the site, the mean for the site can be considered as the mean for an irregular variable [12, 13, 14]. By utilizing the statistical nature of the Hamiltonian, the thermodynamic functions are calculating the average density quantity with respect to the sites, that is,

$$f = [f_i]_{av} \tag{4}$$

where $[f_i]_{av}$ represents the average of f_i.

Figure 3 represents frustration in an irregular system such as an antiferromagnetic lattice. The arrows on the lattice points represent the direction of the spins (± 1), and J_{ij} represents the sign of the interaction. The right side of Equation (4) represents an average operation related to random numbers. This equation is called the self-averaging property. By considering $[f]_{av}$ instead of f, theoretical analysis becomes possible. This average operation is an important concept to be utilized when evaluating the efficiency of a production process.

Strong magnetic order is an order in which spins align in the same direction, and magnetization is the order parameter that characterizes it. We are analyzing the production density flowing through the production process by corresponding it to the order parameter. As a mathematical model, we introduce the convection-diffusion equation. Therefore, we are considering that the ferromagnetic order corresponds to the production density. Table 1 shows a part of the data for Testrun1 in the production flow system. "S1"-"S6" are the working processes. "K1"-"K9" are the workers. "WS" is the standard working time (min) for each process "S1"-"S6", and "Total" is the total working time of "WS" and "S1"-"S6". S_i and S_j correspond to S1-S6, and they are adjacent processes. WS is data obtained mainly as a result of accumulated experience over the course of many years in the production business. It corresponds to the order of the production process and is a variable that leads to the evaluation of work efficiency. The distance between sites r_{ij} is proportional to the waiting time τ_{ij}, where v_{ij} is the speed of movement between sites and τ_{ij} is the waiting time. Therefore, $r_{ij} \propto \tau_{ij}$. The waiting time corresponds to the idle-time given in Appendix A.

Table 1. Testrun1

	WS	S1	S2	S3	S4	S5	S6
K1	15	20	20	25	20	20	20
K2	20	22	21	22	21	19	20
K3	10	20	26	25	22	22	26
K4	20	17	15	19	18	16	18
K5	15	15	20	18	16	15	15
K6	15	15	15	15	15	15	15
K7	15	20	20	30	20	21	20
K8	20	29	33	30	29	32	33
K9	15	14	14	15	14	14	14
Total	145	172	184	199	175	174	181

The physical quantity of spin magnetization per spin m is calculated as the average value of this probability in thermal equilibrium. In the Ising model, the order parameter is related to the magnetization m [12, 13].

Definition 3.1. *Magnetization density*

$$m = \frac{1}{N} \sum_{i}^{N} \langle S_i \rangle \approx \langle S_i \rangle \tag{5}$$

where m is the magnetization density. If the system is uniform, it shows that the magnetization value does not change regardless of where it is.

If the magnetization is defined as in Equation (5), the magnetization will be averaged to zero, making it indistinguishable from the paramagnetic state. Therefore, by taking the square mean of the right side of Equation (5), the magnetization will not be zero [12, 13].

$$q = \frac{1}{N}\sum_{i}^{N} \langle S_i \rangle^2 = \left[\langle S_i \rangle^2 \right]_{av} \tag{6}$$

where q is the spin glass order parameter.

3.2. **Magnetization rate.** The Spin Glass Theory is the theoretical elucidation of the irregularity of magnetization. The free energy of a ferromagnet is determined by the magnetic interactions. Therefore, the free energy of a ferromagnet increases as the magnetic interactions become stronger. We concluded that the measurement of the magnetization rate can be applied to the analysis of the production process.

The magnetization of the Ising model is given by the following equation [12, 13].

$$\chi = \frac{\beta}{N}\sum_{i=1}^{N}\left(1 - \langle S_i \rangle^2\right) = \beta\left(1 - \frac{1}{N}\sum_{i=1}^{N}\langle S_i \rangle^2\right) = \beta(1-q) \tag{7}$$

where χ is the magnetization rate. β is the parameter to determine whether the system is in thermodynamic equilibrium.

Since the spin glass order parameter q is between 0 and 1, the magnetization does not diverge. The reason why the magnetization does not diverge is because the direction of the magnetic field and the direction of the spin are not aligned. Magnetization is a measure of the ease of response of spins to an applied magnetic field. While the field is assumed to be in a constant direction, the order arising from the resulting interactions is different.

Nonlinear magnetization is the magnetization of a material when the local magnetization is finite. It is also known as the spin-glass magnetization [12, 13, 14].

$$\chi_{SG} = \frac{\beta^2}{N}\sum_{i,j=1}^{N}\langle S_i S_j \rangle^2 \tag{8}$$

where χ_{SG} is the spin-glass susceptibility.

The spin glass order phase of spin glasses is in a state where spin inversion symmetry is broken. Therefore, there exists a small magnetic field coordination that breaks it. Here, the local magnetization is

$$m_i = \sum_{\alpha} \mathcal{P}_\alpha m_i^\alpha \tag{9}$$

Figure 5 shows the local magnetization situation. m_i^α and m_i^β are the replica local magnetizations, $\mathcal{P}_\alpha$ is the probability of taking the local magnetization α, and $\mathcal{P}_\beta$ is the probability of taking the local magnetization β. Figure 6 shows the change in the magnetization χ at the transition point T_c. The spin glass order parameter corresponds to the transition point at T_c. Furthermore, for the analysis of the production process, the finite region from T_α to T_β is limited [12, 13]. Therefore, the spin glass order parameter q is

$$q = \frac{1}{N}\sum_{i=1}^{N}\left[\sum_{\alpha,\beta}\mathcal{P}_\alpha\mathcal{P}_\beta m_i^\alpha m_i^\beta\right]_{av} \tag{10}$$

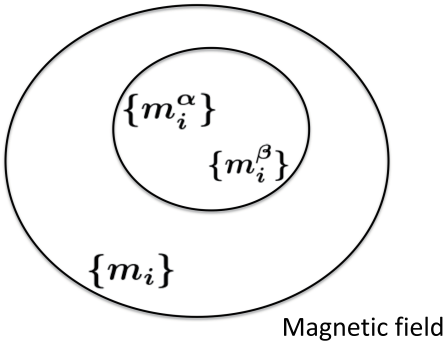

FIGURE 5. Magnetic field

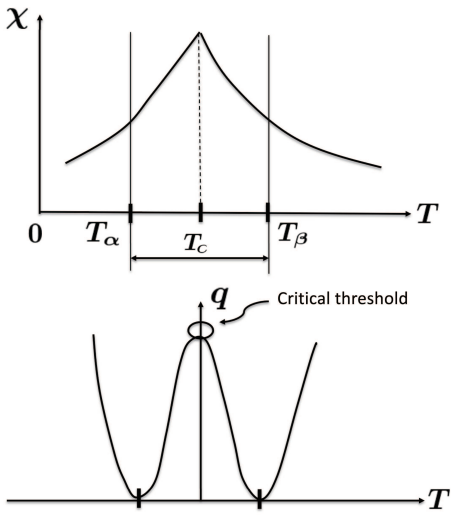

FIGURE 6. Relationship between temperature and magnetization rate and spin glass order parameter

3.3. **Order parameter and Free-energy Landscape of free energy.** In production processes, the same state occurs. The production density varies depending on the process as the production flows. However, the average working time is adopted as a corresponding element of the production density. In the Ising model of strong magnetism, there were only two pure states, but in the case of the spin glass, there are an infinite number of states in which the spins are randomly frozen. This makes a big difference in the thermodynamic properties of the system. If there are an infinite number of pure states, it is appropriate to process them statistically. A pure state refers to a state in which the magnetic state is completely fixed in Spin Glass Theory. In production processes, the working time is not necessarily fixed and irregular. It is viewed as a thermodynamically similar phenomenon. Therefore, the following distribution function is introduced [13, 14].

$$\mathcal{P}(q) = \left[\sum_{\alpha,\beta} \mathcal{P}_\alpha \mathcal{P}_\beta \delta \left(q - \frac{1}{N} \sum_{i=1}^{N} m_i^\alpha m_i^\beta \right) \right]_{av} \tag{11}$$

The order parameter for a spin glass is represented by the mean, so the following equation is obtained [13, 14].

$$q = \int dq' q' \mathcal{P}(q') = \frac{1}{N} \sum_{i=1}^{N} \left[\sum_{\alpha,\beta} \mathcal{P}_\alpha \mathcal{P}_\beta m_i^\alpha m_i^\beta \right]_{av} \tag{12}$$

Taking the average over J_{ij} eliminates the site dependence, and it agrees with Equation (7).

Given the J_{ij}, it is almost impossible to calculate the distribution function and the free energy due to the irregular values of the spin-spin interaction J_{ij}. Therefore, we self-adjust by taking the average of each, that is, the self-averaging of the free energy density. Considering the average of J_{ij} with respect to the production process corresponds to considering the interaction between adjacent processes at the process level [13, 14]. The average free energy is

$$[f]_{av} = -\frac{1}{N\beta} [\ln Z]_{av} \tag{13}$$

The average free energy Z can be calculated by using the following relation to make it easier to handle analytically [13, 14]:

$$Z^n = e^{n \ln Z} = 1 + n \ln Z + \frac{n^2}{2} (\ln Z) + \cdots \tag{14}$$

Then,

$$\ln Z = \lim_{n \to 0} \frac{Z^n - 1}{n} \tag{15}$$

The mean free energy can be obtained by calculating the average of the nth power of the partition function, where n is a natural number [13, 14]. Therefore,

$$[Z^n]_{av} = \left[\mathbf{Tr} e^{-\beta \sum_{a=1}^{n} H(S^a)} \right]_{av} \tag{16}$$

where n is a natural number. The distribution function of the Hamiltonian can be obtained by the replica method. The replica method is a way of determining the state of each part of the system in order to determine the state of the entire system.

3.4. **Mean-field approximation.** Rewrite Equation (16) using the replica method and mean-field approximation to calculate the mean of Z^n.

$$[Z^n]_{av} = \left[\mathbf{Tr} \exp \left(\beta \sum_{\langle ij \rangle} J_{ij} \sum_{a=1}^{n} S_i^a S_j^a \right) \right]_{av}, \quad \beta = \frac{1}{k_\beta T} \tag{17}$$

where the Boltzmann constant k_β and the temperature T are given. The J_{ij} is assumed to be a Gaussian distribution, so the average of J_{ij} is $[J_{ij}]_{av} = 0$, $\left[J_{ij}^2\right]_{av} = J^2$.

By performing the mean operation on Equation (17), i.e., setting the volatility of the Gaussian distribution to J^2, and due to the interaction between replicas generated by the mean operation, we obtain the following equation:

$$[Z^n]_{av} = \mathbf{Tr} \exp \left\{ \frac{\beta^2 J^2}{2} \sum_{\langle ij \rangle} \left(\sum_{a=1}^{n} S_i^a S_j^a \right)^2 \right\} \tag{18}$$

We assume independence for the site regarding the spin-pairing distribution function [13, 14]. When $a \neq b$,

Assumption 3.1.

$$S_i^a S_i^b = q_{ab} + \delta \left(S_i^a S_i^b \right) \tag{19}$$

where q_{ab} is the Free-energy Landscape order parameter.

The second term on the right side represents the deviation from the mean q_{ab}. If the second order term is ignored with respect to the deviation, the following equation is obtained. Refer to the reference for the transformation of the equation [13, 14].

$$\begin{aligned}
[Z^n]_{av} &= \mathbf{Tr} \exp \left(\beta^2 J^2 \sum_{a,b=1(a>b)}^{n} \sum_{\langle ij \rangle} S_i^a S_i^b S_j^a S_j^b + \frac{Nn\beta^2 J^2}{2} \right) \\
&\sim \mathbf{Tr} \exp \left\{ \beta^2 J^2 \sum_{a,b=1(a>b)} \sum_{\langle ij \rangle} \left[q_{ab}^2 + 2 q_{ab} (S_i^a S_i^b - q_{ab}) \right] + \frac{Nnz\beta^2 J^2}{4} \right\} \\
&= \mathbf{Tr} \exp \left(-\frac{Nz}{2} \beta^2 J^2 \sum_{a,b=1}^{n} q_{ab}^2 + z\beta^2 J^2 \sum_{a,b=1(a>b)}^{n} \sum_{i=1}^{N} q_{ab} S_i^a S_i^b + \frac{Nnz\beta^2 J^2}{4} \right)
\end{aligned} \tag{20}$$

where, $a > b$ and N represents the number of atoms that make up the bonds in the molecule, and z represents the coordination number of the atoms. q_{ab} is the canonical average of the mean-field effective Hamiltonian between a and b [13, 14].

$$q_{ab} = \frac{1}{N}\sum_{i=1}^{N}\left\langle S_i^a S_i^b \right\rangle_{\mathit{eff}} \tag{21}$$

where q_{ab} is the order parameter of Free-energy Landscape. $\langle\cdot\rangle_{\mathit{eff}}$ is the canonical average of the mean-field effective Hamiltonian.

Equation (20) represents the mean value of the system's overall state, which is described by the mean-field effective Hamiltonian.

3.5. **Replica-symmetry.** In the Spin Glass Theory, the index dependence of the self-consistent variable q_{ab} is assumed to be the same for all replicas, and the solution is a replica-symmetric $q_{ab} = q$. By verifying the replica-symmetric solutions, the range of application of the Spin Glass Theory to the production process can be clearly defined. The self-consistent variable equation is written as follows with $q_{ab} = q$ [13, 14]:

$$\begin{aligned} q &= \frac{\frac{1}{N}\sum_{i=1}^{N}\mathbf{Tr} S_i^a S_i^b \exp\left(\beta^2 J^2 zq \sum_{c,d=1}^{n}\sum_{i=1}^{N} S_i^c S_i^d\right)}{\mathbf{Tr}\exp\left(\beta^2 J^2 zq \sum_{c,d=1}^{n}\sum_{i=1}^{N} S_i^c S_i^d\right)} \\ &= \frac{\mathbf{Tr} S^a S^b \exp\left[\frac{\beta^2 J^2 zq}{2}\left(\sum_{c,d=1}^{n} S^c\right)^2\right]}{\mathbf{Tr}\exp\left[\frac{\beta^2 J^2 zq}{2}\left(\sum_{c,d=1}^{n} S^c\right)^2\right]}, \quad c > d \end{aligned} \tag{22}$$

Equation (22) is not obvious since there are n types of spins. Let us use an auxiliary variable u to solve this problem by using Gauss integral [13, 14].

$$q = \frac{\int Du \mathbf{Tr} S^a S^b \exp\left(\beta J\sqrt{zq}u \sum_{c=1}^{n} S^c\right)}{\int Du \mathbf{Tr}\exp\left(\beta J\sqrt{zq}u \sum_{c=1}^{n} S^c\right)} \tag{23}$$

where,

$$\int Du(\cdots) = \int_{-\infty}^{\infty}\frac{du}{\sqrt{2\pi}} e^{-\frac{u^2}{2}}(\cdots) \tag{24}$$

Take the spin sum in Equation (23), and take $n \to 0$ [13, 14].

$$\begin{aligned} q &= \frac{\int Du \left(e^{\beta J\sqrt{zq}u} - e^{-\beta J\sqrt{zq}u}\right)^2 \left(e^{\beta J\sqrt{zq}u} + e^{-\beta J\sqrt{zq}u}\right)^{(n-2)}}{\int Du \left(e^{\beta J\sqrt{zq}u} + e^{-\beta J\sqrt{zq}u}\right)^n} \\ &\to \int Du \left(e^{\beta J\sqrt{zq}u} - e^{-\beta J\sqrt{zq}u}\right)^2 \left(e^{\beta J\sqrt{zq}u} + e^{-\beta J\sqrt{zq}u}\right)^{-2} \\ &\quad \left(n \to 0 \quad \mathit{denominator} : \int Du = \int_{-\infty}^{\infty} e^{-\frac{u^2}{2}} du = 1 \to \mathit{denominator} = 1\right) \\ &\quad \left(n \to 0 \quad \mathit{numerator} : \int Du \left(\frac{e^{\beta J\sqrt{zq}u} - e^{-\beta J\sqrt{zq}u}}{e^{\beta J\sqrt{zq}u} + e^{-\beta J\sqrt{zq}u}}\right)^2\right) \\ &\to \int Du \tanh^2\left(\beta J\sqrt{zq}u\right), \quad \left(\frac{e^{\beta J\sqrt{zq}u} - e^{-\beta J\sqrt{zq}u}}{e^{\beta J\sqrt{zq}u} + e^{-\beta J\sqrt{zq}u}} = \tanh\beta J\sqrt{zq}u\right) \end{aligned} \tag{25}$$

Equation (25) is the Free-energy Landscape equation for the spin glass order parameter. Equation (25) always has the solution of $q = 0$. This represents a normal magnetic state.

Figure 7 shows a numerical solution of the Free-energy Landscape equation. Expand the right-hand side of Equation (25).

$$q = \left(\beta J\sqrt{z}\right)^2 q - 2\left(\beta J\sqrt{z}\right)^4 q^2 + \cdots$$
$$q \sim \frac{1}{2}\left(\frac{T}{J\sqrt{z}}\right)\left[1 - \left(\frac{T}{J\sqrt{z}}\right)^2\right] \tag{26}$$

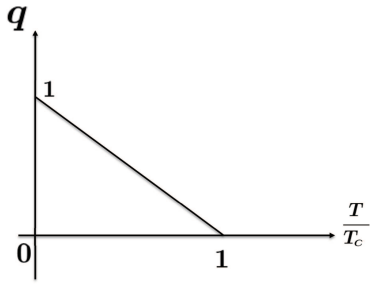

FIGURE 7. Relationship between q and T/T_c

The next transfer temperature T_c is obtained.

$$T_c = J\sqrt{z} \tag{27}$$

At temperatures below the critical temperature T_c, the order parameter q is finite. As the temperature is lowered, q increases and reaches 1 at $T = 0$. To gain insight into the behavior near absolute zero, the self-consistent variable equation is transformed as follows [13, 14]:

$$q = 1 - \int Du \frac{1}{\cosh^2\left(\frac{T_c}{T}\sqrt{q}u\right)} = 1 - \frac{T}{T_c}\int_{-\infty}^{\infty} \frac{dx}{\sqrt{2\pi}} \frac{\exp\left[\frac{-T^2}{2T_c^2}x^2\right]}{\cosh^2\left(\sqrt{q}x\right)} \tag{28}$$

In the second equation of Equation (28), a variable conversion of $u = \frac{T}{T_c}x$ is performed. It can be seen that $T = 0$ will be $q = 1$. Calculate the integral to examine the correction section. Perform integration on Equation (28).

$$q \sim 1 - \frac{T}{T_c}\int_{-\infty}^{\infty} \frac{dx}{\sqrt{2\pi}} \cdot \frac{1}{\cosh^2 x} = 1 - \frac{T}{T_c}\sqrt{\frac{2}{\pi}} \tag{29}$$

where q is the order parameter.

By assuming the replica symmetry solution, the existence of spin glass phase transition was indicated. It is necessary to consider an appropriate region for its application to the production process. Equation (29) is illustrated in Figure 7.

The next thing to verify is that the obtained solution has a non-negative entropy, assuming the replica-symmetric solution in Equation (17) [13, 14].

$$[Z^n] = \mathbf{Tr}\exp\left[-\frac{Nn(n-1)}{4}\beta^2 J^2 z q^2 + \frac{\beta^2 J^2 z q}{2}\sum_{i=1}^{N}\left(\sum_{a=1}^{n} S_i^a\right)^2 - \frac{Nn\beta^2 J^2 z q}{2} + \frac{Nn\beta^2 J^2 z}{4}\right]$$
$$= \exp\left\{\frac{Nn\beta^2 J^2 z}{4}\left[(1-q)^2 - nq^2\right] + N\ln \mathbf{Tr} e^L\right\} \tag{30}$$

The last term of Equation (30) was set as follows:

$$\mathbf{Tr}e^{L} = \mathbf{Tr}\exp\left[\frac{\beta^2 J^2 zq}{2}\left(\sum_{a=1}^{n} S^a\right)^2\right] \tag{31}$$

Proceed in the same way as when taking the spin sum for Equation (25). Then, $n \to 0$,

$$\begin{aligned}\mathbf{Tr}e^{L} &= \int Du\mathbf{Tr}\exp\left(\beta J\sqrt{zq}u\sum_{a=1}^{n} S^a\right)\\ &= \int Du\left(e^{\beta J\sqrt{zq}u} + e^{-\beta J\sqrt{zq}u}\right)^n\\ &\sim 1 + n\int Du\ln\left(e^{\beta J\sqrt{zq}u} + e^{-\beta J\sqrt{zq}u}\right)\end{aligned} \tag{32}$$

Substitute Equation (32) into the expression of the distribution function Equation (13) to calculate the free energy [13, 14].

$$[f]_{av} = -\frac{\beta J^2 z}{4}(1-q)^2 - \frac{1}{\beta}\int Du\ln\left(e^{\beta J\sqrt{zq}u} + e^{-\beta J\sqrt{zq}u}\right) \tag{33}$$

Therefore, the entropy is

$$\begin{aligned}[S]_{av} &= \beta^2\frac{\partial}{\partial\beta}[f]_{av}\\ &= -\frac{\beta^2 J^2 z}{4}(1-q) - \int Du\beta J\sqrt{zq}u\tanh(\beta J\sqrt{zq}u)\\ &\quad + \int Du\ln\left(e^{\beta J\sqrt{zq}u} + e^{-\beta J\sqrt{zq}u}\right)\end{aligned} \tag{34}$$

Further, the second term on the right side of Equation (34) can be manipulated as follows [13, 14]:

$$\int Duuf(u) = -\int Du\frac{\overleftarrow{d}}{du}f(u) = \int Du\frac{d}{du}f(u) \tag{35}$$

We obtain as follows [13, 14]:

$$\begin{aligned}[S]_{av} &= -\frac{\beta^2 J^2 Z}{4}(1-q)^2 - \beta^2 J^2 Zq(1-q) + \int Du\ln\left(e^{\beta J\sqrt{Zq}u} + e^{-\beta J\sqrt{Zq}u}\right)\\ &= -\frac{\beta^2 J^2 Z}{4}(1-q)(1+3q) + \int Du\ln\left(e^{\beta J\sqrt{Zq}u} + e^{-\beta J\sqrt{Zq}u}\right)\end{aligned} \tag{36}$$

The last term of Equation (36) can be ignored when T is small. The main contribution is from the first term of Equation (36). The first term on the right-hand side of Equation (36) is

$$[S]_{av} \sim -\frac{T_c^2}{4T^2}(1-q)(1+3q) \sim -\frac{T_c}{T}\sqrt{\frac{2}{\pi}} \tag{37}$$

Substitute the order parameter q of Equation (29) to Equation (37) and Equation (37) is obtained by ignoring the constant below zero.

Entropy has a negative value at low temperatures and diverges to zero as $T \to 0$. In production processes, this would lead to a state of production stoppage.

$$-\frac{T_c}{T}\sqrt{\frac{2}{\pi}} + \int Du\ln\left(e^{\beta J\sqrt{Zq}u} + e^{-\beta J\sqrt{Zq}u}\right) > 0 \tag{38}$$

When the integral term is sufficiently small, $[S] < 0$. Further analyze the second term of Equation (36) [13, 14].

$$r(u) \approx \int Du \ln\left(e^{ku} + e^{-ku}\right), \quad k = \beta J\sqrt{zq} \tag{39}$$

For entropy to be non-negative, the following equation must be satisfied.

$$\frac{T_c}{T}\sqrt{\frac{2}{\pi}} < r \to T_c < r\sqrt{\frac{2}{\pi}}T, \quad T_c = J\sqrt{z} \tag{40}$$

4. Application of Spin Glass Theory to Production Fields.

4.1. Numerical analysis of the order parameter and the Gaussian integral.

When the order parameter q is $n \to 0$, it becomes Equation (25). On the other hand, the entropy $[S]_{av}$ becomes the left side of Equation (38). Represent the above equation again as follows:

$$q = \int Du \tanh^2(ku), \quad k = \beta J\sqrt{zq} \tag{41}$$

$$[S]_{av} = -\frac{T_c}{T}\sqrt{\frac{2}{\pi}} + \int Du \ln\left(e^{ku} + e^{-ku}\right), \quad k = \beta J\sqrt{zq} \tag{42}$$

In Figure 8, each number represents the following function. Also, in Figure 9, as the volatility σ decreases, the order parameter q increases, indicating that the system approaches a strong ferromagnetic phase. In other words, it shows that there is a large effective energy present.

$$① = \frac{1}{\sqrt{2\pi}\sigma}e^{-\frac{1}{2}\left(\frac{u-\overline{u}}{\sigma}\right)^2}, \quad ② = k^2(u-\overline{u}), \quad ③ = \tanh^2 ku, \quad ④ = ku + m \tag{43}$$

where, when calculating the order parameter q, $k = 1$, $m = 0.5$; when calculating the entropy $[S]_{av}$, $k^2 = 0.1$.

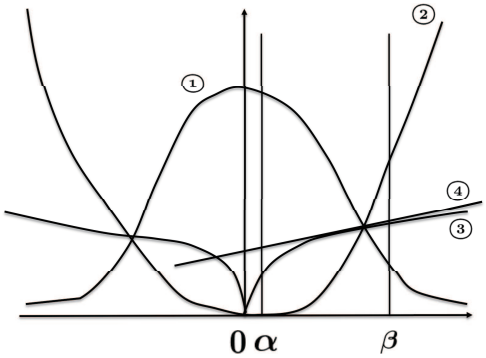

FIGURE 8. A function in a finite domain

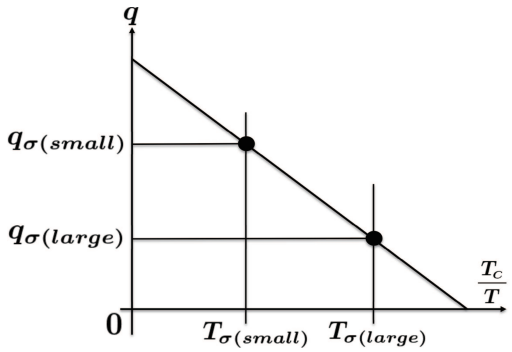

FIGURE 9. Relationship between temparature and order parameters

Approximate Equation (41) and Equation (42) in the following way.

$$\tanh^2(ku) \approx ku + m \tag{44}$$

$$\int Du \ln\left(e^{ku} + e^{-ku}\right) \approx k^2u^2 \tag{45}$$

We do not think it is possible to approximate the function $\tanh^2(ku)$ by a linear approximation, but we judged it to be good for understanding the trend. Therefore,

$$q = \int_{\alpha}^{\beta} \frac{1}{\sqrt{2\pi}\sigma} e^{-\frac{1}{2}\left(\frac{u}{\sigma}\right)^2} \cdot (ku + m)du \tag{46}$$

$$r(u) = \int_{\alpha}^{\beta} \frac{1}{\sqrt{2\pi}\sigma} e^{-\frac{1}{2}\left(\frac{u}{\sigma}\right)^2} \cdot (k^2u^2) \tag{47}$$

At this time, $[S]_{av}$ is as follows:

$$[S]_{av} = r(u) - \frac{T_c}{T}\sqrt{\frac{2}{\pi}} \tag{48}$$

From Table 2 and Figure 9, it can be seen that when $\sigma \to small$, $q \to large$. Therefore, when $q \to large$, $T_c/T \to large$, which indicates that there is a large effective energy when σ is small, i.e., at low temperatures. However, from Table 2, we can read the numerical trends, although the $[S]_{av}$ value of $\mu = 0.1$, $\sigma = 0.05$ (56.277) is larger than that of $\mu = 0.4$, $\sigma = 0.05$ (55.086) due to the error of approximation. Table 2 shows the values in the range from 0 to β, which is a positive value close to 0. It indicates the values of the right half of the integral value. The smaller the σ, the closer it is to the ferromagnetic phase, which is equivalent to the irregularity of the spin interaction being small and the spins being in the same direction. If fitted into the production process, $\sigma \to large$ corresponds to Testrun1, and $\sigma \to small$ corresponds to Testrun2. Figure 10 shows that if the volatility $\sigma > 0.4$, there is an unsatisfactory part. As k^2 increases, $r(u)$ will naturally become larger. $r(u)$ is less than $+\infty$ and is a positive finite value. Figure 11 shows the variation of $f(u)$ and $g(u)$ with the change of σ and k^2.

$$f(u) = \frac{1}{\sqrt{2\pi}} e^{-\frac{1}{2}\left(\frac{\mu}{\sigma}\right)^2}, \quad g(u) = k^2u^2 \tag{49}$$

TABLE 2. Compare Testrun1 with Testrun2

	<Testrun1>, $\sigma = 0.27$		<Testrun2>, $\sigma = 0.05$	
μ	q	$[S]_{av}$	q	$[S]_{av}$
0.8	25.073	53.731	23.6	58.807
0.4	27.119	49.082	27.8	55.086
0.1	8.898	47.182	9.7	56.277

As shown in Figure 12, S_i and S_j represent the spin states, and J_{ij} is the interaction between S_i and S_j, which is only between adjacent spins. The working time data is shown in Table 6 (Testrun1) or Table 8 (Testrun2) in Appendix A.

$$r(u) > \frac{T_c}{T}\sqrt{\frac{2}{\pi}} \Rightarrow T > \frac{T_c}{r(u)}\sqrt{\frac{2}{\pi}} \Rightarrow T_c < \sqrt{\frac{\pi}{2}} r(u)T \tag{50}$$

Apply the values in Table 3. Then,

$$\begin{aligned} T_{0.02} &> \frac{T_c}{183}\sqrt{\frac{2}{\pi}} = 0.005T_c\sqrt{\frac{2}{\pi}} \\ T_{0.23} &> \frac{T_c}{107}\sqrt{\frac{2}{\pi}} = 0.009T_c\sqrt{\frac{2}{\pi}} \end{aligned} \tag{51}$$

This means that the higher the temperature, the higher the energy. Therefore, $T_{0.23} > T_{0.02}$. Compared to $\sigma = 0.23$, $\sigma = 0.02$ has a larger effective energy for the same T_c. From

Figure 13, the magnitude of magnetization is $q_{0.02} > q_{0.23}$, and the strength of the magnet pole is stronger for $\sigma = 0.02$ than for $\sigma = 0.23$. The strength of the magnet pole can be thought of as the strength of the economic field (production field).

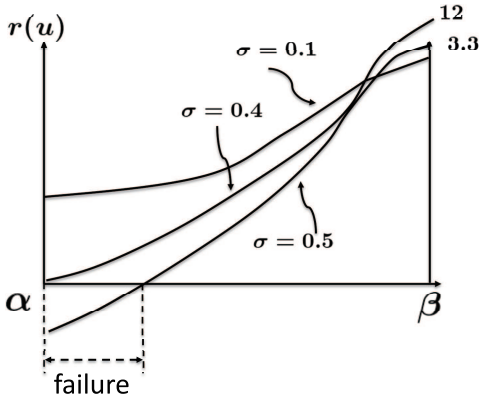

FIGURE 10. Value of $r(u)$

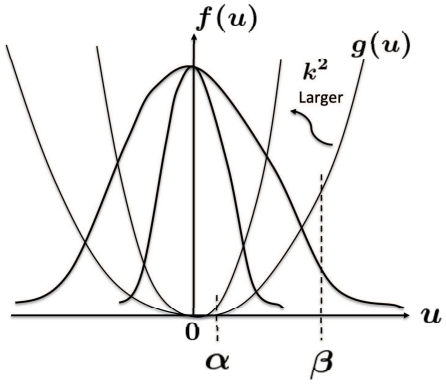

FIGURE 11. Value of $f(u)$, $g(u)$

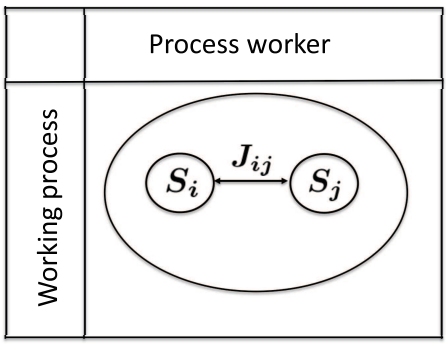

FIGURE 12. Classification by type

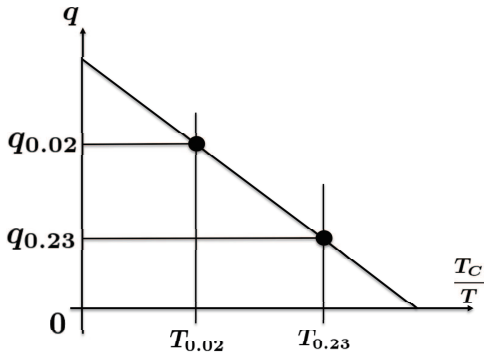

FIGURE 13. Strength of magnetization

TABLE 3. Spin glass phase

$\sigma = 0.02$	$k^2 = 1$	$r(u) \fallingdotseq 183$
$\sigma = 0.23$	$k^2 = 1$	$r(u) = 107$

4.2. **Assumption of a limited domain.**

$$q = \int Du \left[\tanh^2\left(\beta J\sqrt{Zq}u\right)\right]$$
$$[S]_{av} \cong -\frac{T_c}{T}\sqrt{\frac{2}{\pi}} + \int Du \left[\ln\left(e^{ku} + e^{-ku}\right)\right], \quad \int Du[\bullet] = \int_{\alpha}^{\beta} \frac{1}{\sqrt{2\pi}\sigma} e^{-\frac{1}{2}\left(\frac{u}{\sigma}\right)^2},$$
$$k = \beta J\sqrt{Zq} \tag{52}$$

Now, Maclaurin expansion of $\tanh x$ is as follows:

$$\tanh x = x - \frac{1}{3}x^3 + O\left(x^5\right) \approx x - \frac{1}{3}x^3 \tag{53}$$

In the first-order approximation of $\tanh x$, it is expressed as $\tanh x \sim kx + m$, and in the third-order approximation, it is expressed as $\tanh x \sim k\left(x - \frac{1}{3}x^3\right)$.

In Figure 8, $q : g(u) = 2u + 0.2$ is an appropriate approximation for the left half area of the ① function, and $r(u) > \frac{T_c}{T}$, where T_c and T are constants. That is, $T > \frac{T_c}{r(u)}\sqrt{\frac{2}{\pi}}$, $[S]_{av} > 0$ and $r(u) - \frac{T}{T_c}\sqrt{\frac{2}{\pi}} > 0$.

From the above calculation, it can be seen that when σ is small, q becomes larger. Therefore, when q is larger, T/T_c becomes larger, which means that in a system with a small σ, there is a large effective energy due to the temperature. As mentioned above, the smaller the σ, the closer the phase is to the ferromagnetic phase, which means that the irregularity of the spin interaction is small and the spins are assumed to be in the same direction.

Regarding the integral $\int_a^b g(x)f(x)dx$, if $f(x)$ is the probability density function of a normal distribution and $g(x)$ is a first or second order equation in x, especially in the case of a first order equation, let the integral value be denoted as $G(x)$, such as Figure 14.

$$G(x) = (p\mu + d)\Phi\left(\frac{U-\mu}{\sigma}\right) - (p\mu + d)\Phi\left(\frac{L-\mu}{\sigma}\right) - P\alpha\left\{\varphi\left(\frac{U-\mu}{\sigma}\right) - \varphi\left(\frac{L-\mu}{\sigma}\right)\right\} \tag{54}$$

Let $k = L/U$, and when the calculation is performed, if $k < 1$, then $\mu < 1$, which gives the figure in the text and the calculated value. However, this is only the case when $\mu > 0$ and $\mu < 1$, which is the case for the ferromagnetic phase [16]. Figure 15 shows the transition with respect to the variable u of the order parameter q as an example. The setting parameters are $\sigma = 0.27$, $\mu = 0.8$ in Table 2. Figure 16 shows the transition with respect to a certain range of variation of the entropy S_{av} as an example. The setting parameters are $\sigma = 0.27$, $\mu = 0.8$ in Table 2. Table 4 is a correspondence table between the strength of magnetism in Spin Glass Theory and the synchronism of production flow systems.

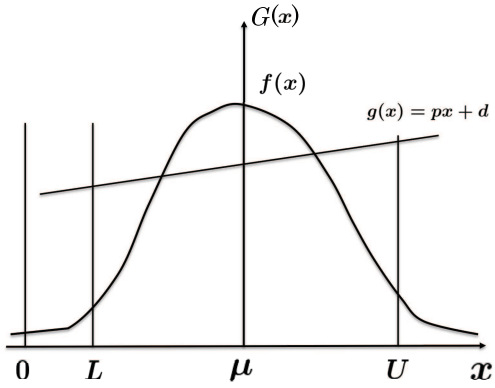

FIGURE 14. Function in a finite domain

5. **Production Business of a Small-to-Midsize Firm.**

5.1. **Production systems in the production equipment industry.**

We refer to the production system in manufacturing equipment industry studied in this paper. This is not a special system, but "Make-to-order system with version control". Make-to-order system is a system which allows necessary manufacturing after taking orders from clients, resulting in "volatility" according to its delivery date and lead time. In addition, "volatility" occurs in lead time depending on the contents of make-to-order products (production equipment).

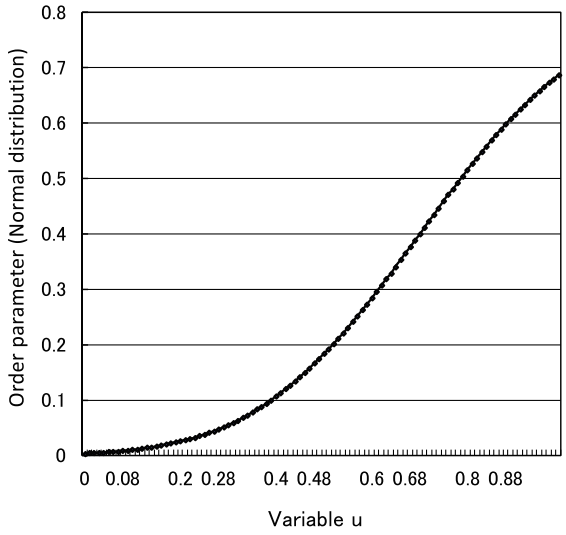

FIGURE 15. Order parameter (Normal Distribution), $\sigma = 0.27$, $\mu = 0.8$

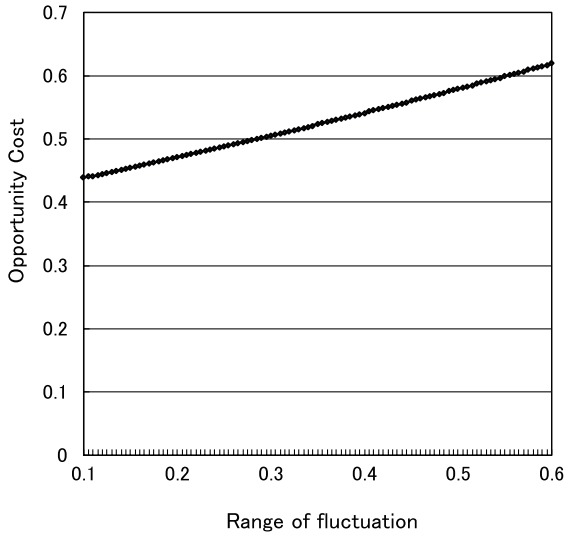

FIGURE 16. Loss of opportunity (Entropy Value), $\sigma = 0.27$, $\mu = 0.8$

TABLE 4. Correspondence between Spin Glass Theory and production method

Spin Glass Theory	Production method
Ferromagnetic material	Synchronous production method
Weakly magnetic body	Asynchronous production method

However, effective utilization of the production forecast information on the orders may suppress certain amount of "variation", but the complete suppression of variation will be difficult. In other words, "volatility" in monthly cash flow occurs and of course influences a rate of return in these companies. Production management system, suitable for the separate make-to-order system which is managed by numbers assigned to each product upon order, is called as "product number management system" and is widely used. All productions are controlled with numbered products and instructions are given for each numbered product.

Thus, ordering design, logistics and suppliers are conducted for each manufacturer's serial numbers in most cases except for semifinished products (unit incorporated into the final product) and strategic stocks. Therefore, careful management of the lead time or production date may not suppress "volatility" in manufacturing (production). The company in this study is the "supplier" in Figure 17 and "factory" here. In Figure 17(A), the "Customer side" refers to an ordering company and "Supplier (D)" means the target company in this paper. The product manufacturer, which is the source of the ordered production equipment presents an order that takes account of the market price. In Figure 17(B), the market development department at the customer's factory receives the order through the sale contract based on the predetermined strategy. This is the data actually measured by Customer and Manufacturer (to be researched) shown in Figure 17. It presents the production process data that received an order for a particular customer out of several existing customers. The client is a major semiconductor manufacturer. We have a long history of producing equipment.

5.2. **Production flow system.** A manufacturing process that is termed as a production flow process is shown in Figure 18. The production flow process, which manufactures low

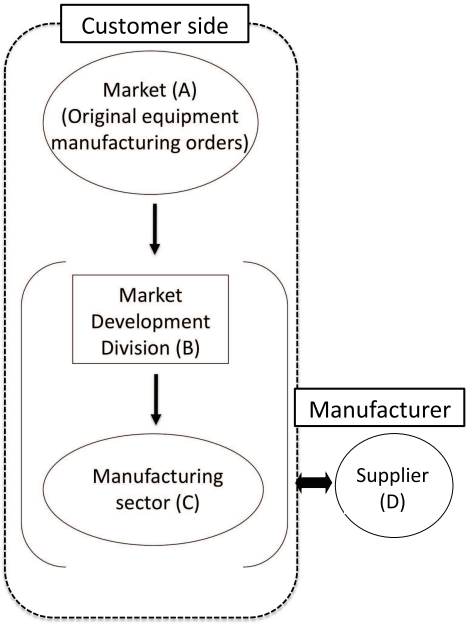

FIGURE 17. Business structure of the target company

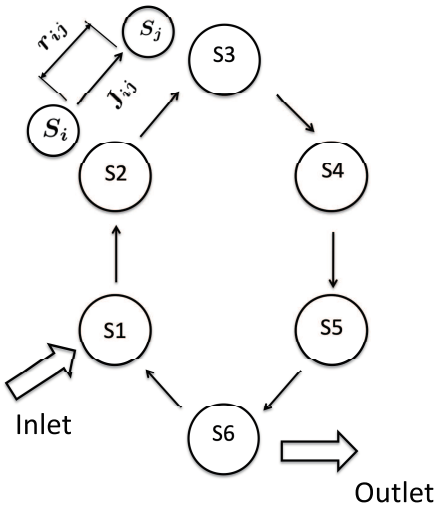

FIGURE 18. Production flow process

volumes of a wide variety of products, is produced through several stages in the production process. In Figure 18, the processes consist of six stages. The adjacent processes S_i and S_j in the production flow system correspond to the spin-spin glass order J_{ij} in Equation (1). r_{ij} in Equation (1) is the adjacent working interval when moving from adjacent process S_i to S_j. In each step S1-S6 of the manufacturing process, materials are being produced by one worker of each step S1 through S6. S1-S6, which are given by Tables 6 and 8 in Appendix A, correspond to the process in Figure 18. The throughput will vary greatly depending on the proficiency level of the worker (Testrun1 and Testrun2 in Appendix A). Testrun1 and Testrun2 are an asynchronous process and a synchronous process, respectively. The direction of the arrow represents the direction of the production flow. In this system, production materials are supplied from the inlet and the end product will be shipped from the outlet.

Assumption 5.1. *The production structure is nonlinear.*

Assumption 5.2. *The production structure is a closed structure; that is, the production is driven by a cyclic system (production flow system).*

- Reasonability of Assumption 5.1. Assumption 5.1 indicates that the determination of the production structure is considered a major factor, which includes the generation value of production or the rate of return generation structure in a stochastic manufacturing process (hereafter called the manufacturing field). Because such a structure is at least dependent on the demand, it is considered to have a nonlinear structure. Because the value of such a product depends on the rate of return, its production structure is nonlinear. Therefore, Assumption 5.1 reflects the realistic production structure and is somewhat valid.
- Reasonability of Assumption 5.2. Assumption 5.2 is completed in each step and flows from the next step until stage S6 is completed. Assumption 5.2 is reasonable because new production starts from S1. A more detailed analysis, please refer to our Appendix A.

6. **Conclusion.** In the Spin Glass Theory, the irregularity of spins is assumed to be small and the spins at each site are assumed to be in the same direction, which means approaching the ferromagnetic phase. This ferromagnetic phase is represented by the efficient synchronous production method, Testrun2. Specifically, by calculating the spin glass order parameter and entropy in Spin Glass Theory, it was concluded that the synchronous production system is the best production system in the production flow systems. For future research, we are considering the relationship between phase transitions in spin glass space and phase transitions in production systems.

REFERENCES

[1] K. Shirai, Y. Amano, A. Ando and T. Uda, Optimizing sales and profit processes using impulse control, *International Journal of Innovative Computing, Information and Control*, vol.17, no.6, pp.1887-1905, 2021.

[2] K. Shirai, Y. Amano and T. Uda, Manufacture allocation of the batch process and the cyclic flow process via stochastic analysis, *International Journal of Innovative Computing, Information and Control*, vol.16, no.3, pp.939-954, 2020.

[3] K. Shirai, Y. Amano and T. Uda, Cost reduction function considering stochastic risks in the production process, *International Journal of Innovative Computing, Information and Control*, vol.16, no.4, pp.1257-1278, 2020.

[4] K. Shirai, Y. Amano, A. Ando and T. Uda, Evaluation of production flow system utilizing expected high volume effective rate, *International Journal of Innovative Computing, Information and Control*, vol.17, no.4, pp.1203-1224, 2021.

[5] K. Shirai, Y. Amano and A. Ando, Analytical mechanics approach to conservation in production field, *International Journal of Innovative Computing, Information and Control*, vol.17, no.1, pp.67-91, 2021.

[6] K. Shirai, Y. Amano, A. Ando and T. Uda, Securing a synchronization zone to realize a high efficiency production based on the generalized theory of relativity, *International Journal of Innovative Computing, Information and Control*, vol.19, no.1, pp.101-121, 2023.

[7] K. Shirai, Y. Amano, A. Ando and T. Uda, Analysis of the throughput of the production system with the aid of general relativity, *International Journal of Innovative Computing, Information and Control*, vol.18, no.4, pp.1071-1088, 2022.

[8] K. Shirai and Y. Amano, Use of a Riemannian manifold to improve the throughput of a production flow system, *International Journal of Innovative Computing, Information and Control*, vol.12, no.4, pp.1073-1087, 2016.

[9] K. Shirai, Y. Amano, A. Ando and T. Uda, Spatial properties of production flow system based on Riemannian manifold structure, *International Journal of Innovative Computing, Information and Control*, vol.17, no.3, pp.831-851, 2021.

[10] H. Tasaki, *Thermodynamics – From a Modern Perspective (New Physics Series, Japanese)*, Baifukan Co., Ltd., 2000.

[11] K. Hayama and H. Irie, Trial production of kite wing attached multicopter for power saving and long flight, *ICIC Express Letters, Part B: Applications*, vol.10, no.5, pp.405-412, 2019.

[12] K. Nemoto, Statistical mechanics approach to probabilistic information processing, *The Results of the Special Research Area of the Grant-in-Aid for Scientific Research*, 2002 (Presentation).

[13] K. Takahashi and H. Nishimori, *Phase Transition and Critical Phenomena in Entangled Groups*, Maruzen Publishing Co., Ltd., 2017.

[14] M. Suzuki, *Statistical Mechanics*, Iwanami Shoten Co., Ltd., 2002.

[15] Hogeeson, *Spin Glass Theory and Far Beyond*, World Scientific Publishing Co., Inc., 2023.

[16] K. Shirai and Y. Amano, Analysis of production processes using a lead-time function, *International Journal of Innovative Computing, Information and Control*, vol.12, no.1, pp.125-138, 2016.

Appendix A: Analysis of Actual Data in the Production Flow System. For many years, we have been involved in the manufacture of a certain major semiconductor manufacturing equipment in Kyoto. Fortunately, we have been able to create our current production process by continuing to manufacture advanced equipment. We have also manufactured optimal temperature control equipment for plastic greenhouses.

Regarding with Testrun1 (Table 6) and Testrun2 (Table 8), the production process starts at S1 and ends at S6, as shown in Figure 18. This process is repeated to complete the production unit, where K1 to K9 represent the workers involved in the production. The data in Table 6 and Table 8, except for WS, represent the work time (min) involved in the manufacture of a particular device.

Based on the control equipment, the product can be manufactured in one cycle. The rate of return required to maintain 6 pieces of equipment/day is as follows.

- (Testrun1): Because the throughput of each process (S1-S6) is asynchronous, the overall process throughput is asynchronous. In Table 5, we list the manufacturing time (min) of each process. In Table 7, we list the volatility in each process performed by the workers. Finally, Table 6 lists the target times. The theoretical throughput is obtained as $3 \times 199 + 2 \times 15 = 627$ (min). In addition, the total working time in stage S3 is 199 (min), which causes a bottleneck. In Figure 19, we plot the measurement data listed in Table 6, which represents the total working time of each worker (K1-K9). In Figure 20, we plot the data contained in Table 6, which represents the volatility of the working times.

Table 5. Correspondence between the table labels and the Testrun number

	Table number	Production process	Working time	Volatility
Testrun1	Table 6	Asynchronous process	627 (min)	0.29
Testrun2	Table 8	Synchronous process	500 (min)	0.06
Testrun3	Table 10	"Synchronization with preprocess" method	400 (min)	0.03

Table 6. Testrun1

	WS	S1	S2	S3	S4	S5	S6
K1	15	20	20	25	20	20	20
K2	20	22	21	22	21	19	20
K3	10	20	26	25	22	22	26
K4	20	17	15	19	18	16	18
K5	15	15	20	18	16	15	15
K6	15	15	15	15	15	15	15
K7	15	20	20	30	20	21	20
K8	20	29	33	30	29	32	33
K9	15	14	14	15	14	14	14
Total	145	172	184	199	175	174	181

Table 7. Volatility of Table 6

	S1	S2	S3	S4	S5	S6
K1	1.67	1.67	3.33	1.67	1.67	1.67
K2	2.33	2	2.33	2	1.33	1.67
K3	1.67	3.67	3.33	2.33	2.33	3.67
K4	0.67	0	1.33	1	0.33	1
K5	0	1.67	1	0.33	0	0
K6	0	0	0	0	0	0
K7	1.67	1.67	5	1.67	2	1.67
K8	4.67	6	5	4.67	5.67	6
K9	0.33	0.33	0	0.33	0.33	0.33

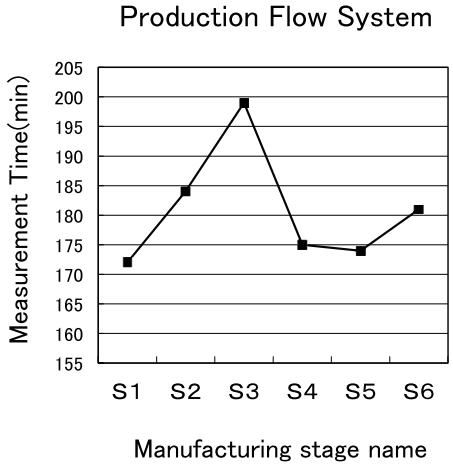

FIGURE 19. Total work time for each stage (S1-S6) in Table 6

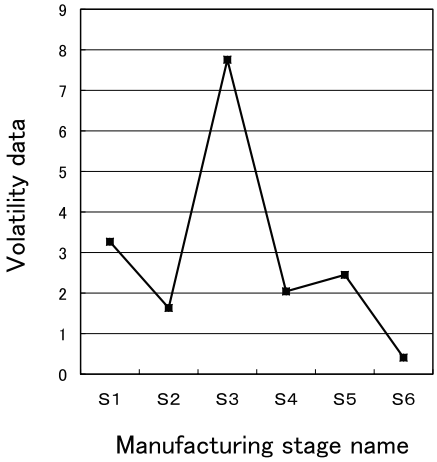

FIGURE 20. Volatility data for each stage (S1-S6) in Table 6

- (Testrun2): Set to synchronously process the throughput. The target time listed in Table 8 is 500 (min), and the theoretical throughput (not including the synchronization idle time) is 400 (min). Table 9 presents the volatility of each working process (S1-S6) for each worker (K1-K9).

TABLE 8. Testrun2

	WS	S1	S2	S3	S4	S5	S6
K1	20	20	24	20	20	20	20
K2	20	20	20	20	20	22	20
K3	20	20	20	20	20	20	20
K4	20	25	25	20	20	20	20
K5	20	20	20	20	20	20	20
K6	20	20	20	20	20	20	20
K7	20	20	20	20	20	20	20
K8	20	27	27	22	23	20	20
K9	20	20	20	20	20	20	20
Total	180	192	196	182	183	182	180

TABLE 9. Volatility of Table 8

	S1	S2	S3	S4	S5	S6
K1	0	1.33	0	0	0	0
K2	0	0	0	0	0.67	0
K3	0	0	0	0	0	0
K4	1.67	1.67	0	0	0	0
K5	0	0	0	0	0	0
K6	0	0	0	0	0	0
K7	0	0	0	0	0	0
K8	2.33	2.33	0.67	1	0	0
K9	0	0	0	0	0	0

- (Testrun3): Introduce a preprocess stage. The process throughput is performed synchronously with the reclassification of the process. As shown in Table 10, the theoretical throughput (not including the synchronization idle time) is 400 (min). Table 11 presents the volatility of each working process (S1-S6) for each worker (K1-K9). On the basis of these results, the idle time must be set to 100 (min). Moreover, the theoretical target throughput (T_s') can be obtained using the "Synchronization with preprocess" method. This goal is as follows:

$$\begin{aligned} T_s &\sim 20 \times 6 \text{ (First cycle)} + 17 \times 6 \text{ (Second cycle)} \\ &\quad + 20 \times 6 \text{ (Third cycle)} + 20 \text{ (Previous process)} + 8 \text{ (Idle-time)} \\ &\sim 370 \text{ (min)} \end{aligned} \tag{55}$$

The full synchronous throughput in one stage (20 min) is

$$T_s' = 3 \times 120 + 40 = 400 \text{ (min)} \tag{56}$$

This real data (Testrun3) is an example of manufacturing one product in three cycles: First cycle is 20×6 (min), Second cycle is 17×6 (min), and Third cycle is 20×6 (min). Previous process means a process that can be processed in advance before being put into the production flow process. Idle-time is the waiting time of 8 (min) for the process that occurred throughout the three cycles. The total is 370 (min). This total work time is 10% more efficient than Testrun2 (400 min).

TABLE 10. Total manufacturing time at each stage for each worker, K5(*): Preprocess

	WS	S1	S2	S3	S4	S5	S6
K1	20	18	19	18	18	18	18
K2	20	18	18	18	18	18	18
K3	20	21	21	21	21	21	21
K4	16	13	11	11	13	13	13
K5	16	*	*	*	*	*	*
K6	16	18	18	18	18	18	18
K7	16	14	14	13	14	14	13
K8	20	22	22	22	22	22	22
K9	20	20	20	20	20	20	20
Total	148	144	143	141	144	144	143

TABLE 11. Volatility of Table 10, K5(*): Preprocess

	S1	S2	S3	S4	S5	S6
K1	0.67	0.33	0.67	0.67	0.67	0.67
K2	0.67	0.67	0.67	0.67	0.67	0.67
K3	0.33	0.33	0.33	0.33	0.33	0.33
K4	1	1.67	1.67	1	1	1
K5	*	*	*	*	*	*
K6	0.67	0.67	0.67	0.67	0.67	0.67
K7	0.67	0.67	1	0.67	0.67	1
K8	0.67	0.67	0.67	0.67	0.67	0.67
K9	0	0	0	0	0	0

Using the "Synchronization with preprocess" method, the throughput is reduced by approximately 10%. Therefore, we showed that our proposed "Synchronization with preprocess" method is realistic and can be applied in production flow systems. Below, we represent for a description of the "Synchronization with preprocess".

Next, we manufactured one piece of equipment in three cycles. To maintain a throughput of six units/day, the production throughput must be as follows:

$$\frac{(60 \times 8 - 28)}{3} \times \frac{1}{6} \simeq 25 \text{ (min)} \tag{57}$$

where the throughput of the preprocess is set to 20 (min). In Equation (57), the value 28 represents the throughput of the preprocess plus the idle-time for synchronization. Similarly, the number of processes is 8 and the total number of processes is 9 (8 plus the preprocess). The value of 60 is obtained as 20 (min) $\times$ 3 (cycles).

The results are as follows. Here, the trend coefficient, which is the actual number of pieces of equipment/the target number of equipment, represents a factor that indicates the degree of the number of pieces of manufacturing equipment.
Testrun1: 4.4 (pieces of equipment)/6 (pieces of equipment) = 0.73,
Testrun2: 5.5 (pieces of equipment)/6 (pieces of equipment) = 0.92,
Testrun3: 5.7 (pieces of equipment)/6 (pieces of equipment) = 0.95.
Volatility data represent the average value of each Testrun.

Appendix B: Table to Summarize Figures in This Paper except for Appendix A.

TABLE 12. Title of figures

Figure number	Title name of figure
Figure 1	State of spin coordination
Figure 2	Spin table
Figure 3	An example of a spin arrangement in a ferromagnetic material
Figure 4	Free-energy Landscape
Figure 5	Magnetic field
Figure 6	Relationship between temperature and magnetization rate and spin glass order parameter
Figure 7	Relationship between q and T/T_c
Figure 8	A function in a finite domain
Figure 9	Relationship between temparature and order parameters
Figure 10	Value of $r(u)$
Figure 11	Value of $f(u)$, $g(u)$
Figure 12	Classification by type
Figure 13	Strength of magnetization
Figure 14	Function in a finite domain
Figure 15	Order parameter (Normal Distribution), $\sigma = 0.27$, $\mu = 0.8$
Figure 16	Loss of opportunity (Entropy Value), $\sigma = 0.27$, $\mu = 0.8$
Figure 17	Business structure of the target company
Figure 18	Production flow process

Appendix C: Table to Summarize Formulas in This Paper except for Appendix A.

TABLE 13. Title of equations

Equation number	Title name of equation
Equation (1)	Spin-spin interaction
Equation (2)	Hamiltonian H of the nearest-neighbor interaction
Equation (3)	Thermodynamic function as the average density with respect to sites
Equation (4)	Thermodynamic function as the mean for the site
Equation (5)	Magnetization density
Equation (6)	Spin glass order parameter
Equation (7)	Magnetization of the Ising model
Equation (8)	Spin-glass magnetization
Equation (9)	Local magnetization
Equation (10)	Spin glass order parameter
Equation (11)	Distribution function
Equation (12)	Order parameter for a spin glass represented by the mean
Equation (13)	Thermodynamic function
Equation (14)	Average free energy
Equation (15)	Average free energy Z
Equation (16)	Mean free energy
Equation (17)	Rewrite Equation (16)
Equation (18)	Mean value on Equation (17)
Equation (19)	Assuming equation of independence for the site
Equation (20)	Average free energy Z
Equation (21)	Canonical average of the mean-field effective Hamiltonian
Equation (22)	Self-consistent variable equation
Equation (23)	Equation for the auxiliary variable u to solve this problem by using Gauss integral
Equation (24)	Gauss integral equation
Equation (25)	Spin glass order parameter
Equation (26)	Expand the right-hand side of Equation (25)
Equation (27)	Transfer temperature
Equation (28)	The self-consistent variable equation that is transformed from Equation (26)
Equation (29)	Performing integration on Equation (28)
Equation (30)	Replica-symmetric solution in Equation (17)
Equation (31)	Last term of Equation (30)
Equation (32)	Spin sum for Equation (25)
Equation (33)	Calculation equation from Equation (32) and Equation (13)
Equation (34)	Entropy equation
Equation (35)	Second term on the right side of Equation (34)
Equation (36)	Entropy equation same as Equation (34)
Equation (37)	First term on the right-hand side of Equation (36)
Equation (38)	Entropy equation
Equation (39)	$r(u)$ equation
Equation (40)	Entropy equation to be non-negative
Equation (41)	Spin glass order parameter
Equation (42)	Entropy equation
Equation (43)	Example of each function in Figure 8
Equation (44)	Function $\tanh^2(ku)$ by a linear approximation
Equation (45)	Approximation of $\int Du \ln\left(e^{ku} + e^{-ku}\right)$
Equation (46)	Function $\tanh^2(ku)$ by a linear approximation
Equation (47)	Equation $r(u)$
Equation (48)	Equation $[S]_{av}$
Equation (49)	Equation $f(u)$
Equation (50)	Inequality of $r(u)$
Equation (51)	Inequality of $T_{0.02}$ and $T_{0.23}$
Equation (52)	Approximation of Equation $[S]_{av}$
Equation (53)	Approximation of function $\tanh x$
Equation (54)	Calculation equation of $G(x)$

Author Biography

Kenji Shirai received the B.Sc. degree in Electrical Engineering from Ritsumeikan University, Japan, 1973; the M.Sc. degree in Electrical Engineering from Ritsumeikan University, Japan, 1975; the Ph.D. degree in Electrical Engineering from Ritsumeikan University, Japan, 2000.

Dr. Shirai is engaged in research on optimal control of distributed parameter systems, modeling of industrial systems applying mathematical finance, and optimal control.

Yoshinori Amano received the B.Sc. degree in Electrical Engineering from Ritsumeikan University, Japan, 1971; the M.Sc. degree in Electrical Engineering from Ritsumeikan University, Japan, 1973; the Ph.D. degree in Electrical Engineering from Ritsumeikan University, Japan, 1977.

Dr. Amano is engaged in research on optimal control of distributed parameter systems, modeling of information systems applying mathematical finance, and optimal control. Currently, he is an Advisor of Kyohnan Elecs Co., Ltd.

Atsuya Ando received the Dr. Eng. degree in System Information Engineering from Tsukuba University, in 2013. In 1990, he joined the Nippon Telegraph and Telephone Corporation (NTT) Wireless Systems Laboratories, Yokosuka, Japan. He was engaged in research and development of personal and base station antennas for wireless mobile communication systems. From 2000 to 2003, he was with the ATR Adaptive Communications Research Laboratories, Kyoto, Japan, engaging in research and development on adaptive array antennas for wireless ad-hoc network systems. In 2019, he moved to Niigata University of International and Information Studies, and he is currently a Professor in the Department of Information Systems, Faculty of Business and Informatics. His research interests include mobile and base station antennas using metamaterials for wireless communication systems.

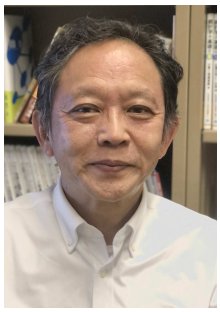

Takayuki Uda received a doctoral degree (Information Science) from the Graduate School of Information Sciences, Tohoku University, Japan, in 2009; a master's degree (Informatics) from the University of Library and Information Science (now Information and Media Studies, University of Tsukuba).

Dr. Uda is currently a full-time Professor at the Department of Information Systems, Faculty of Business and Informatics, Niigata University of International and Information Studies. His research fields are data science and natural language processing. His research results contribute to the education and research of students.